JETIR.ORG ISSN: 2349-5162 | ESTD Year : 2014 | Monthly Issue
JOURNAL OF EMERGING TECHNOLOGIES AND INNOVATIVE RESEARCH (JETIR)
An International Scholarly Open Access, Peer-reviewed, Refereed Journal

Design and analysis of polarization independent multiband meta-material absorber for defence applications

Surbhi[1], Abhinv Kumr[2], Rohit Kumr[3], Prashant Kumar[4]

Bhagalpur College of Engineering, Bhagalpur, Bihar, India

Abstract

An ultra-thin, quad-band metamaterial absorber with high absorptivity in each operating band is given in this study. The proposed structure is made up of a square ring, a circular split ring, and four inner symmetric quadrants printed on a 1.6mm thick FR4 substrate. The simulated outcome demonstrates that under normal incident electromagnetic conditions, the quad-band metamaterial absorber achieves high absorbance of 99.58%, 99.85%, 99.91%, and 99.55% at 7.04GHz, 8.13 GHz, 10.91GHz, and 12.54GHz respectively. The absorber has a symmetrical design and exhibits polarization-insensitive behaviour under normal incidence. Additionally, it exhibits high absorption for wide incident angles up to 45 for both transverse electric and magnetic polarizations. Surface current distribution is used to analyze the absorption mechanism of different parts of the proposed metamaterial absorber (MMA). The designed quad band absorber can be used in C and X band applications.

1. Introduction

Metamaterial structures are artificially engineered structures with unique electromagnetic properties that are not found in nature [1]. The distinct features of metamaterials are derived from their newly designed structures rather than the features of the base materials. They have extraordinary features such as negative permittivity, permeability, negative refractive index, etc. that allow them to manipulate electromagnetic waves in ways beyond what is achievable with ordinary materials. Typically, metallic unit cells are arranged periodically on a dielectric layer to create metamaterial structures. Invisibility cloaks [2], antennas [3], filters [4], spectroscopy [5] and sub-wavelength imaging [6] are some of the applications of metamaterial. Designing ideal MMAs is one of the main usages.

Metamaterial absorbers are such devices that can efficiently absorb electromagnetic waves (EM). It is typically a sandwiched structure, consisting of a resonator on the top side of the substrate and backed with a highly conductive metallic ground plane. It consists of three functional layers which have different roles in realizing the perfect absorption. The top side of the absorber is electrically excited at resonance frequency. On the other hand, the magnetic field excitation has been established in the dielectric substrate (middle layer) because of the circulating current in the upper and lower layers in opposite directions. The copper layer at the bottom does not transmit any incident power through it. The electric and magnetic field excitation varies the effective permittivity and effective permeability of the structure in such a way that the input impedance of the absorber matches with free space impedance. When electric and magnetic resonance occur simultaneously, high absorption is achieved.

The study of MMA is gaining momentum due to the various benefits that it offers over conventional ones, including its ultra-thin nature, wide incidence angle absorption, polarization insensitivity, and simple unit cell design. A metal-dielectric-metal sandwich structure was implemented by Landy et al. in 2008 to demonstrate the first microwave metamaterial absorber [7]. Since then, many metamaterial absorbers have been studied to show their superior qualities with single-band, dual-band, multi-band and broadband operations. Due to the fact that high-absorption MMAs with a single band are ineffective in a number of applications, broad-band or high-performance MMAs with multiple bands and compact dimensions need to be investigated.

Multiband metamaterial absorbers provide perfect absorption at a number of distinct frequencies. Two approaches are commonly employed to design a multiband MMA. The first approach, often referred to as the coplanar construction method involves combining several resonators of different sizes to form a superunit structure [8, 9]. Vertical stacking of alternating multi-layer structures is another approach [10, 11]. But neither of these methods is ideal to obtain a structure that offers multiband absorption. While the layered design approach could not completely overcome the disadvantage of the heavy weight and large thickness of the structure, coplanar construction necessarily results in an expansion of MMA unit size. In order to achieve multi-band absorption, certain simplified structural designs were recently put out.

This paper suggests a polarization-insensitive, ultrathin, quad-band metamaterial absorber with wide-angle absorption properties. The suggested design consists of four inner symmetric quadrants, a square ring, and a circular split ring. The simulated result displays four discrete absorption peaks at 7.04GHz, 8.13 GHz, 10.91GHz, and 12.54GHz with peak absorptivities of 99.58%, 99.85%, 99.91%, and 99.55% respectively. Since the MMA is symmetrical, its absorption is unaffected by different polarization angles. Additionally, it exhibits significant absorption for wide incident angles up to 45º for both transverse electric and transverse magnetic polarizations.

2. Theoretical Background

The absorptivity A(ω) of MMA when plane wave strikes it is calculated by equation (1) [12],where S_{11}, $S_{21}$and A(ω) represent the reflection coefficient, transmission coefficient and absorptivity respectively at angular frequency ω.

$$A(\omega) = 1 - |S_{11}|^2 - |S_{21}|^2 \quad (1)$$

Since the bottom layer is entirely copper laminated, therefore $|S_{21}|^2 \to 0$ and now absorption fully relies on $|S_{11}|^2$.To produce high absorption, reflection should be minimum, which is accomplished when impedance of the proposed absorber matches with that of free space.

3. Unit Cell Geometry

Fig.1 (b) shows the proposed MMA structure which consists of a top metallic patterned layer, a dielectric layer, and a bottom ground plane. The top layer is made up of copper which consists of an outer square ring, a circular split ring, and four inner symmetric quadrants as displayed in Fig.1 (a). The middle layer is made up of FR4 substrate (relative permittivity εr =4.2 and loss tangent tanδ=0.02 with a thickness of 1.6mm) which serves as a dielectric. Copper (σ=5.8 × 10^7) with a thickness of 0.035mm is used for both the top and bottom layers.

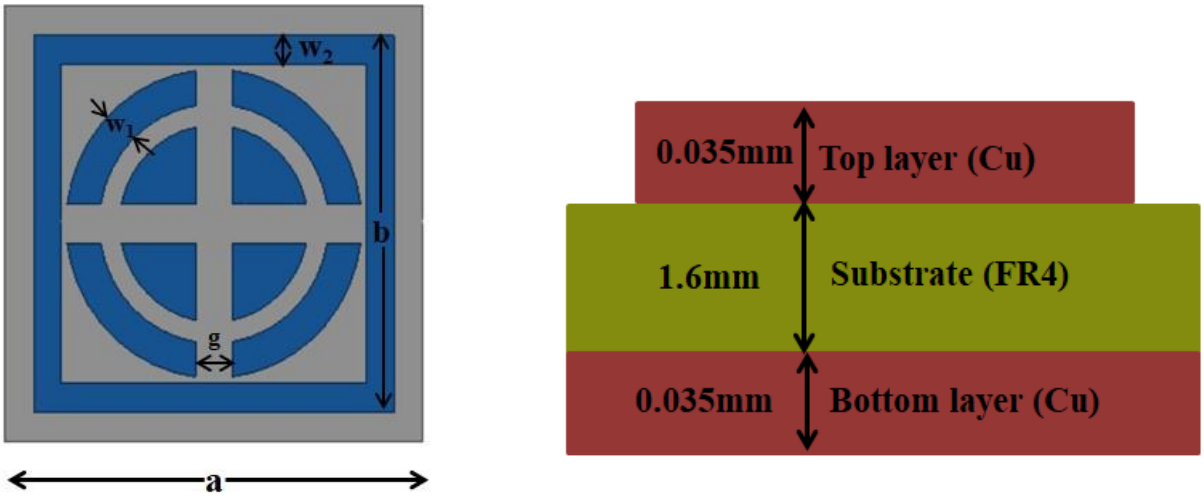

(a) **(b)**

Figure 1 (a) Top view of unit cell and (b) Three-layer design of the proposed structure

The full-wave EM simulation is carried out in Ansys HFSS and Fig. 2 displays the simulated absorptivity of the suggested absorber. The proposed metamaterial absorber provides four distinct absorption peaks at 7.04 GHz, 8.13GHz, 10.91GHz, and 12.54 GHz with absorptivities of 99.58%, 99.85%, 99.91% ,and 99.55% respectively.

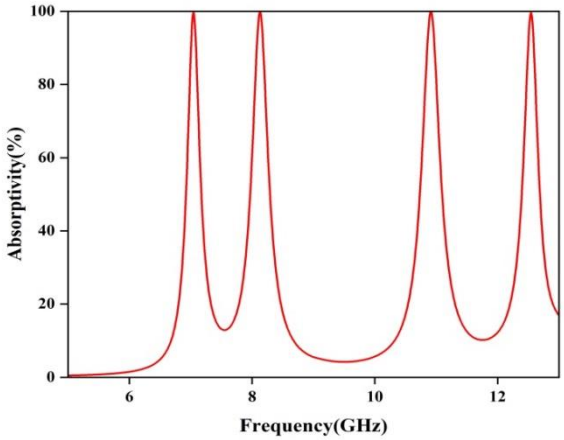

Figure 2 Simulated absorptivity of proposed absorber

4. Design Evolution

As shown in Figure 3, there are multiple stages involved in designing the proposed MMA unit cell. Two absorption peaks are obtained in the unit cell consisting only outer square ring. Absorption is roughly 51% at 7.21 GHz and 99.77% at 10.72 GHz. Adding a circular split ring in unit cell design not only increases the number of bands but also leads to higher amplitude absorption peaks. This new design produces three resonant peaks which are observed at 6.99 GHz, 8.03 GHz, and 10.88 GHz, with absorptivity of 99.8%, 99.34%, and 97.87% respectively. The design is further modified by inserting four symmetric quadrants within the circular split ring and it results in four absorption peaks at 7.04GHz, 8.13GHz, 10.91GHz, and 12.54GHz, all of which cover the C and X bands.

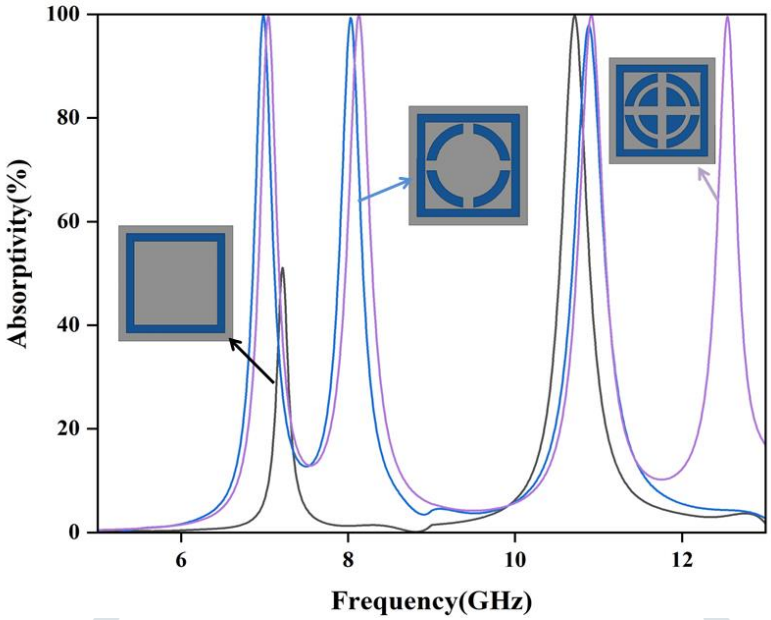

Figure3. Absorptance for various designing steps towards proposed unit cell.

5. Parametric Study

This section is focused on the relationship between several MMA geometric parameters and the absorption spectrum. A trial-and-error technique is used to choose each of the geometrical parameters of the proposed structure until the desired result is achieved. Ansys HFSS simulates the structure with periodic boundary conditions.

5.1 Length of the unit cell

The length of the unit cell (a) is changed from a=22.4 mm to a=22.8 mm in Fig 4 and their absorptivity is examined. It can be observed that the best result is obtained at a=22.6mm.

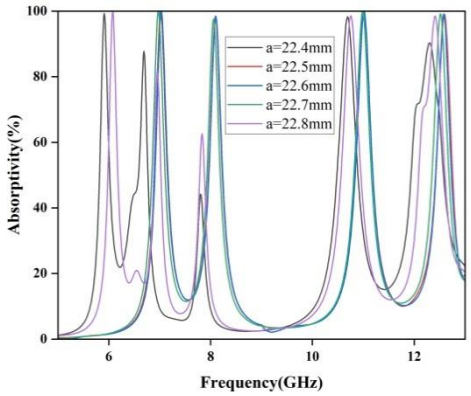

Figure 4 Absorption for various changes in length of unit cell (a)

5.2 Length of square ring resonator

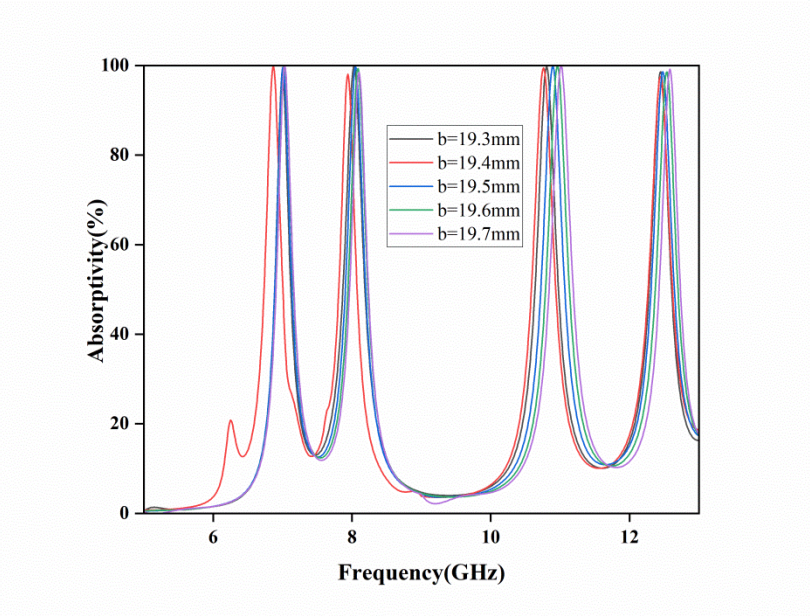

Figure 5 Absorption for various changes in length of square ring resonator (b)

The length of the square ring (b) is varied from b=19.3 mm to b=19.7 mm and their absorptivity response is depicted in Fig.5.. The best result is obtained at b=19.5 mm.

5.3 Width of Circular split ring

In Fig. 6, the width of a circular split ring is varied from w_1=1.5mm to w_1=2.0mm and their absorptivity response is analyzed. It can be noticed that the best result is achieved at w_1=1.8mm.

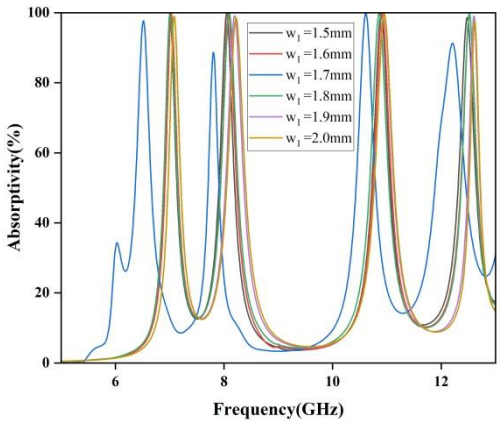

Figure 6 Absorption for various changes in width of circular split ring (w_1)

5.4 Width of square ring resonator

The width of square ring resonator (w_2) is varied from 1.3mm to 1.7 mm by keeping a step size of 0.1mm. Its absorption response is depicted in Fig. 7. From this figure, it can be stated that the best result is obtained at w_2=1.5mm.

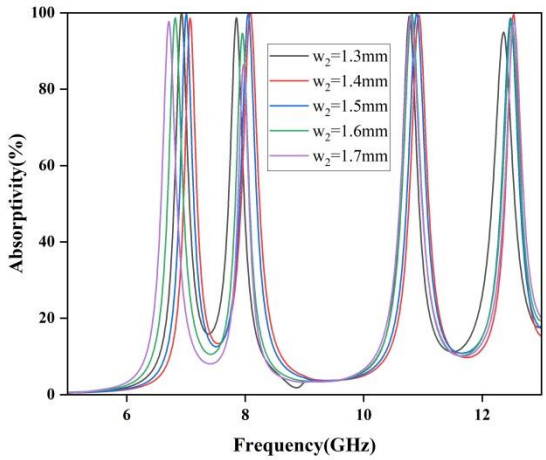

Figure 7 Absorption for various changes in width of square ring resonator (w_2)

5.5 Split gap of circular ring

The split gap (g) of the circular ring is changed from g=1.8mm to g=2.2mm and its absorption response is plotted in Fig.8.It can be noticed that the best outcome is achieved at g=2.0mm. From Fig. 8, it can be observed that the absorption peaks in each band occur at higher frequencies for higher values of g. As g decreases, the absorption peak frequencies shift towards the lower values. The splits in the circular ring behave like parallel plate capacitors with a thickness of 0.035mm and placed at a distance of g. The capacitance is increased by lowering the split gap distance which in turn reduces the resonance frequencies and this causes the absorption peaks to shift towards lower frequencies.

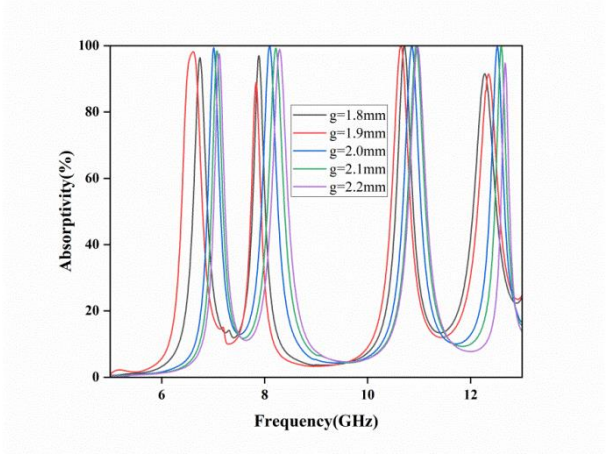

5.6 Radius of inner circular disc (r)

The inner circular disc radius (r) is varied from 4.9mm to 5.3mm and their absorptivity is shown in Fig. 9. From the figure, it can be observed that the best result is obtained at r=5.1mm. Four symmetric quadrants are formed by removing two rectangular slabs from the inner circular disc of radius r.

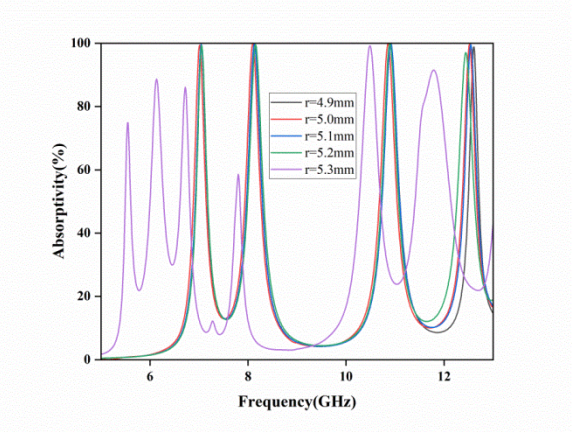

Figure 9 Absorptance for change in radius of inner circular disc(r)

6. Absorption mechanism

The absorption mechanism of perfect absorbers depends on electric and magnetic resonances which in turn vary the effective permittivity and permeability of metamaterial for achieving impedance matching with free space. In such a case, there is no reflection at the interface and thus the entire incident power has a chance to be absorbed inside the metamaterial absorber.

The absorptivity can be calculated by eqn. (1) where S_{11} and S_{21} are the reflection and transmission coefficients respectively. As the bottom layer is completely copper laminated, the incident power cannot transmit through it, i.e., S_{21} becomes zero, and absorption fully depends on S_{11} parameters. A low value of S_{11} indicates better absorption in MMA.

$$A(\omega) = 1 - |S_{11}|^2 - |S_{21}|^2 \quad (1)$$

The reflection coefficient can also be stated in terms of the effective impedance of the absorber by using the eqn. (2) [13], where Z_{eff} is the effective impedance of MMA and Z_0 is free space impedance.S_{11} is minimum when the impedance of the absorber matches with free space impedance. Impedance of absorber can be expressed in terms of its permittivity and permeability by eqn. (5) [14]. Free space impedance and Normalized impedance (Z) can be determined by eqn. (3) [14] and (4) [14] respectively.

$$S_{11} = \frac{Z_{eff} - Z_0}{Z_{eff} + Z_0} \quad (2)$$

$$Z_0 = \sqrt{\frac{\mu_0}{\varepsilon_0}} = 377 ohm \quad (3)$$

$$Z = \frac{Z_{eff}}{Z_0} \quad (4)$$

$$Z_{eff} = \sqrt{\frac{\mu_0 \mu_{eff}}{\varepsilon_0 \varepsilon_{eff}}} = Z_0 \sqrt{\frac{\mu_{eff}}{\varepsilon_{eff}}} = Z_0 \sqrt{\frac{\mu + j\mu'}{\varepsilon + j\varepsilon'}} \quad (5)$$

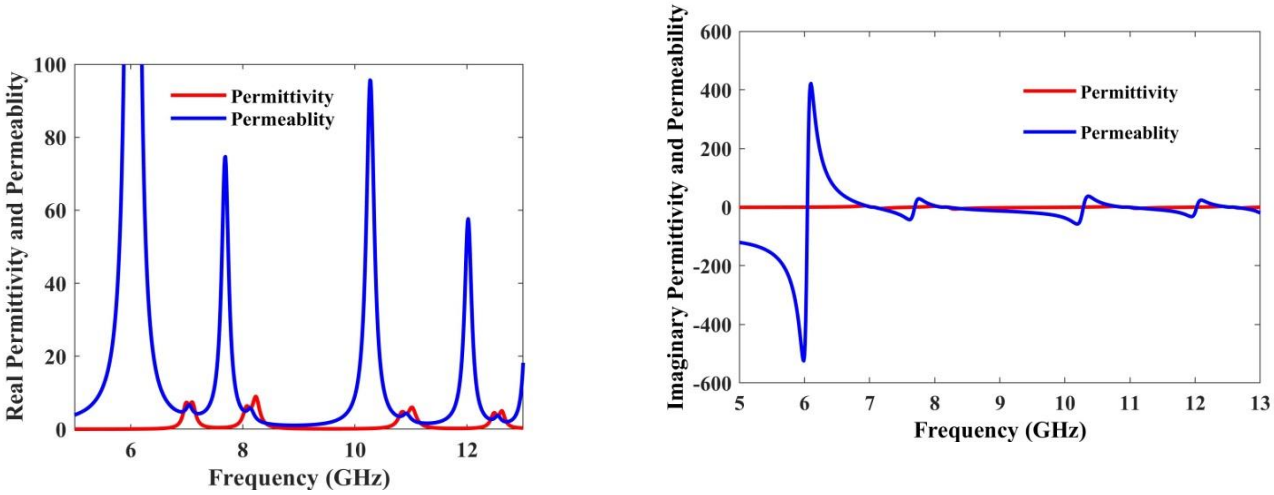

(a) **(b)**

Figure 10(a) Real part of ε_{eff} and μ_{eff} of proposed absorber **(b)** Imaginary part of ε_{eff} and μ_{eff} of proposed absorber

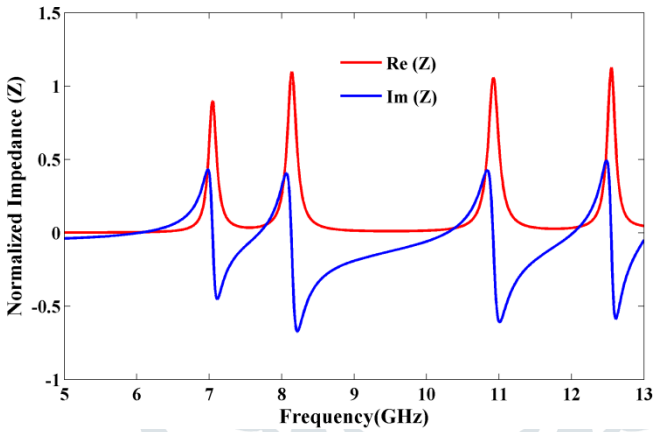

Figure 11 Impedance of proposed absorber

From Fig.11, it can be seen that at absorption peaks, the real and imaginary parts of normalized input impedance become unity and zero, respectively. Normalized impedance approaches unity when the real part of permittivity and permeability of the absorber becomes equal and the imaginary part of permittivity and permeability become zero as shown in Fig.10.It indicates proper impedance matching of absorber with free space which results in maximum absorption. To further examine the absorption process, surface current density distributions on the top and bottom metallic layers corresponding to four absorption peaks are shown in Fig.12. At 7.04 GHz, the surface current is mostly concentrated in the outer square ring and intermediate circular split ring whereas the majority of the current is distributed in the intermediate circular split ring at 8.13 GHz Surface current is mainly localised in outer square ring at 10.91GHz.On the other hand, it is distributed in all resonators at 12.54 GHz.

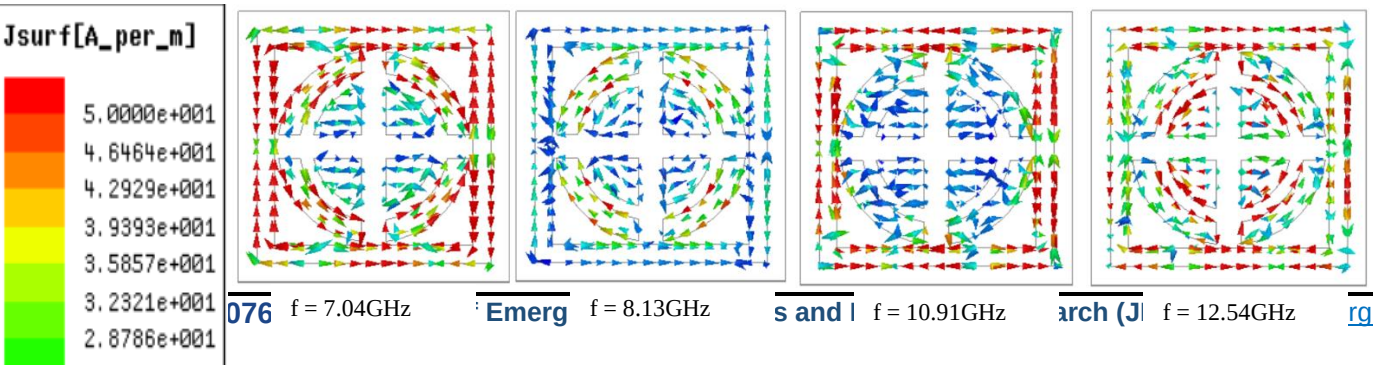

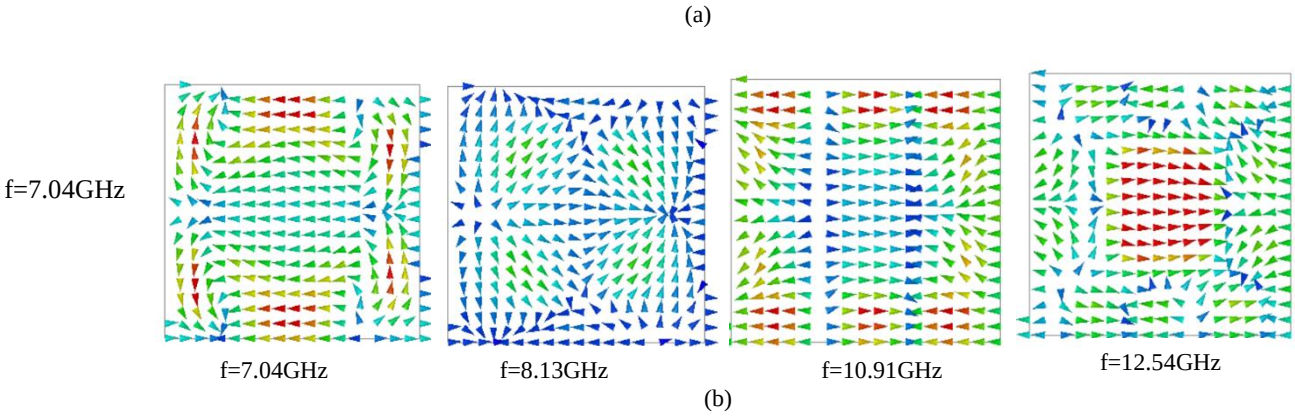

Figure 12 Surface current distributions at resonance frequencies on (a) top layer (b) bottom layer

.At all four absorption frequencies, the top and bottom surface currents flow in an antiparallel direction forming a circulating loop around the incident magnetic field which results in magnetic excitation. On the other hand, the incident electric field electrically excites the metallic patch array on the upper surface. Maximum absorptivity is achieved when electric and magnetic excitation occurs simultaneously.

7. Polarization Insensitive behaviour

7.1 Normal Incidence

The proposed structure is examined for both normal and oblique incidence. It is polarization insensitive under normal incidence due to the symmetrical structure of the designed absorber. In order to verify the polarization performance of the proposed absorber, the propagation direction of the electromagnetic wave is held constant while the electric and magnetic field directions rotate at different polarization angles (Φ) with a step size of 15º. It can be observed that the absorption of MMA remains stable for polarization angles ranging from 0º to 90º as shown in Fig.13.

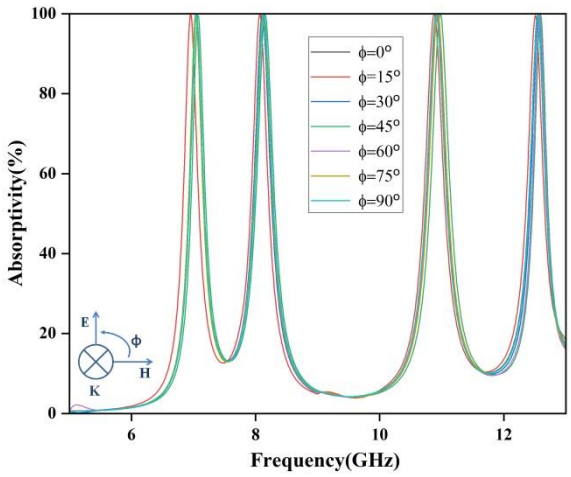

Figure 13 Simulated absorptivities for different polarization angles

7.2 Oblique Incidence

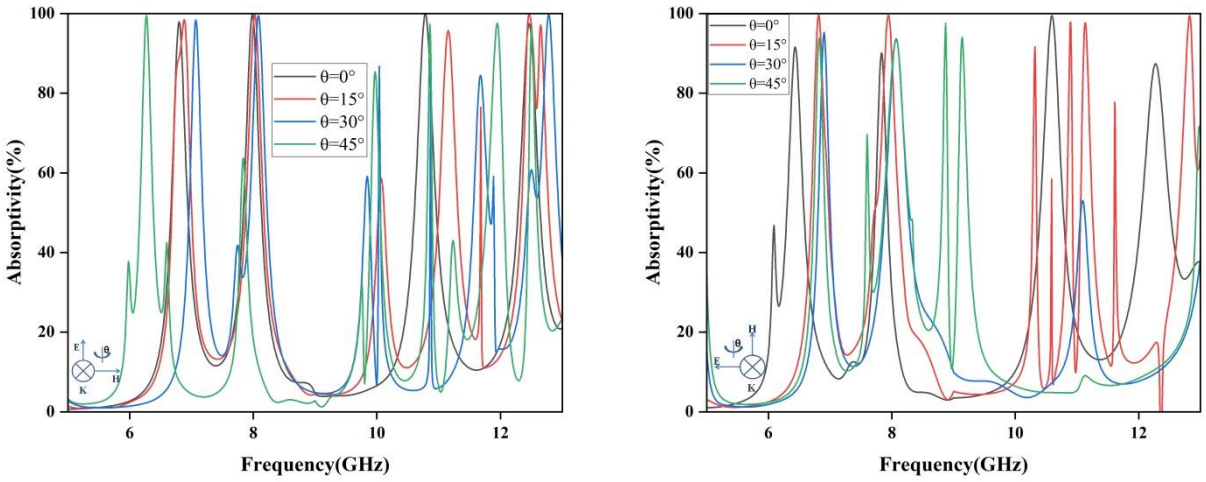

Figure 14 Simulated absorptivity of the proposed absorber at different incident angles for the (a) TE and (b) TM polarizations

Under oblique incident of wave, the proposed structure is studied for both TE and TM polarization. In the case of TE polarization, the direction of wave propagation and magnetic field direction rotates at various incidence angles whereas the E-field direction is kept constant. In TM polarization, the direction of wave propagation and electric field direction rotates at various incidence angles whereas the H-field direction is kept constant. The proposed structure is simulated at different incidence angles (0º to 45º) for both TE and TM polarization. It can be observed that absorptivity is still greater than 80% in both cases for all four resonant frequencies as shown in Fig. 14.

TABLE 1. Comparison of the proposed MMA with previously proposed multiband MMA.

Reference	Size of unit cells	Packing or type of unit cell	Material	Resonances frequency(GHz) & Peak Absorptance	Thickness (mm)	Normal incidence	Oblique angle incidence	
[15]	$0.27\lambda_o \times 0.27\lambda_o$	Square	FR-4, Copper	2.24GHz (97.2%), 7GHz (98%)	$0.0119\lambda_o$	Not mentioned	Not mentioned	Not mentioned
[16]	$0.20\lambda_o \times 0.20\lambda_o$	Square	FR-4, Copper	4.4GHz (94.03%), 6.2GHz (96.61%), 14.2GHz (99.47%)	$0.0147\lambda_o$	Polarization Insensitive	A(ω)>90% upto 45°	A(ω)>90% upto 45º
[17]	$0.32\lambda_o \times 0.32\lambda_o$	Square	FR-4, Copper	8.7GHz (98.14%), 9.25GHz (99.45%), 9.93GHz (98.22%)	$0.0465\lambda_o$	Polarization Insensitive	Maintain 50% absorbance up to 50º	Maintain 50% absorbance up to 50º
[18]	$0.33\lambda_o \times 0.33\lambda_o$	Square	FR-4, Copper	5.92GHz (98.56%), 6.64GHz (97.83%), 10.88GHz (99.61%), 12.87GHz (99.77%)	$0.0197\lambda_o$	Polarization Insensitive	A(ω)>60% upto 60º	A(ω)>60% upto 60º

[19]	$0.106\lambda_o \times 0.106\lambda_o$	Square	FR-4, Copper	4.1GHz (97.9%), 6.86GHz (99.1%), 11.3GHz (99.5%), 13.45Hz (99.95%)	$0.0205\lambda_o$	Polarization Insensitive	Not mentioned	Not mentioned
[20]	$0.50\lambda_o \times 0.50\lambda_o$	Square	FR-4, Copper	6.8GHz (97.2%), 8.24GHz (95.2%), 11.24GHz (97.7%), 12.7GHz (98.5%)	$0.0363\lambda_o$	Polarization Insensitive	A(ω)>90% upto 40º	A(ω)>90% upto 40º
Proposed	$0.53\lambda_o \times 0.53\lambda_o$	Square	FR-4, Copper	7.04GHz (99.58%), 8.13GHz (99.85%), 10.91GHz (99.91%), 12.54GHz (99.55%)	$0.0375\lambda_o$	Polarization Insensitive	A(ω)>80% upto 45º	A(ω)>80% upto 45º

Conclusion

In this paper, a polarization-insensitive quad-band metamaterial absorber has been proposed. Geometric dimensions of the suggested structure are optimized to obtain high absorptivity of 99.58%, 99.85%, 99.91%, and 99.55% at 7.04GHz, 8.13 GHz, 10.91GHz, and 12.54GHz respectively. The proposed MMA has a thickness of $0.0375\lambda o$ at the lowest resonant frequency which is significantly thinner than the conventional absorber. Surface current distributions and normalized input impedance have been examined for a better understanding of the absorption mechanism. The symmetry of the unit cell structure of the design has resulted in polarization insensitivity. The proposed absorber has been compared with previously published multiband MMA in Table 1. It has been observed that the proposed absorber structure has the highest absorptivity at all four resonant frequencies. Additionally, the structure exhibits high absorption for both TE and TM polarizations at a range of incidence angles (0º to 45º). With a simple design and high absorptivity, the suggested absorber can be used in stealth technology, radome, and satellite communication.

Acknowledgement

References

[1] Gangwar, Amit, and S. C. Gupta. "Metamaterials—A new era of artificial materials with extraordinary properties." *International Journal of Engineering Research and Management Technology* 1.2 (2014): 76-84.

[2] Schurig, David, et al. "Metamaterial electromagnetic cloak at microwave frequencies." *Science* 314.5801 (2006): 977-980.

[3] Lu, Chunchi, et al. "Multi-target continuous-wave vital sign radar using 24 GHz metamaterial leaky wave antennas." *2019 IEEE MTT-S International Microwave Biomedical Conference (IMBioC)*. Vol. 1. IEEE, 2019.

[4] Martín, Ferran, et al. "METAMATERIAL-INSPIRED BALANCED FILTERS." *Balanced Microwave Filters* (2018): 353-371.

[5] Liu, X. L., L. P. Wang, and Z. M. Zhang. "Wideband tunable omnidirectional infrared absorbers based on doped-silicon nanowire arrays." *Journal of Heat Transfer* 135.6 (2013): 061602.

[6] Zhao, Junming, et al. "Sub-wavelength image manipulating through compensated anisotropic metamaterial prisms." *Optics Express* 16.22 (2008): 18057-18066.

[7] Landy, N. Iê, et al. "Perfect metamaterial absorber." *Physical review letters* 100.20 (2008): 207402.

[8] Xu, Jianping, et al. "Frequency-tunable metamaterial absorber with three bands." *Optik* 172 (2018): 1057-1063.

[9] Ma, Ben, et al. "Novel three-band microwave metamaterial absorber." *Journal of Electromagnetic Waves and Applications* 28.12 (2014): 1478-1486.

[10] Hu, Fangrong, et al. "Design of a polarization insensitive multiband terahertz metamaterial absorber." *Journal of Physics D: Applied Physics* 46.19 (2013): 195103.

[11] Wang, Ben-Xin, et al. "Six-band terahertz metamaterial absorber based on the combination of multiple-order responses of metallic patches in a dual-layer stacked resonance structure." *Scientific reports* 7.1 (2017): 41373.

[12] Ayop, Osman, et al. "Triple band circular ring-shaped metamaterial absorber for x-band applications." *Progress In Electromagnetics Research M* 39 (2014): 65-75.

[13] Li, Si-Jia, et al. "Ultra-wideband and polarization-insensitive perfect absorber using multilayer metamaterials, lumped resistors, and strong coupling effects." *Nanoscale research letters* 13 (2018): 1-13.

[14] Barde, Chetan, Arvind Choubey, and Rashmi Sinha. "Wide band metamaterial absorber for Ku and K band applications." *Journal of Applied Physics* 126.17 (2019).

[15] Edries, Mohamed, et al. "Simulation design of dual band metamaterial absorber based on the fractal structure." *2019 IEEE International Symposium on Antennas and Propagation and USNC-URSI Radio Science Meeting*. IEEE, 2019.

[16] Zeng, Xianliang, et al. "Design of a triple-band metamaterial absorber using equivalent circuit model and interference theory." *Microwave and Optical Technology Letters* 60.7 (2018): 1676-1681.

[17] Fan, Shicheng, and Yaoliang Song. "Bandwidth-enhanced polarization-insensitive metamaterial absorber based on fractal structures." *Journal of Applied Physics* 123.8 (2018).

[18] Sood, Deepak, and Chandra Charu Tripathi. "Quad band electric field-driven LC resonator-based polarisation-insensitive metamaterial absorber." *IET Microwaves, Antennas & Propagation* 12.4 (2018): 588-594.

[19] Moniruzzaman, Md, et al. "Quad band metamaterial absorber based on asymmetric circular split ring resonator for multiband microwave applications." *Results in Physics* 19 (2020): 103467.

[20] Ren, Yu-Hui, et al. "Design of a quad-band wide-angle microwave metamaterial absorber." *Journal of Electronic Materials* 46 (2017): 370-376.